THE ASTROPHYSICAL JOURNAL, 318:145–160, 1987 July 1

THE ULTRAVIOLET AND OPTICAL EMISSION-LINE SPECTRUM OF III Zw 77[1]

GARY J. FERLAND[2]
Astronomy Department, The Ohio State University
AND
DONALD E. OSTERBROCK
Lick Observatory and Board of Studies in Astronomy and Astrophysics, University of California, Santa Cruz
Received 1986 August 27; accepted 1986 December 9

ABSTRACT

The high-ionization Seyfert 1 galaxy III Zw 77 has been simultaneously observed over the satellite ultraviolet to near-infrared spectral regions. The continuous energy distribution is similar to other active nuclei in that it shows a roughly power-law decline across much of the optical region, and a flatter-than-unity spectral index in the near-ultraviolet ($\lambda \leq 1500$ Å). The equivalent widths of the Balmer lines and Lyα are very similar to those found in other active nuclei, such as those in the samples of Shuder and Wu, Boggess, and Gull, suggesting that III Zw 77 is a "normal" active nucleus, and that its lines should be interpreted in terms of photoionization equilibrium rather than as a special case. The ultraviolet to optical emission-line spectrum for the narrow lines is fairly similar to those deduced for Seyfert 2 galaxies, in which the emitting gas is also thought to be photoionized. A surprising result of our study is the detection of the O III] λ1661, 1666 doublet with an intensity, relative to the optical [O III] lines, suggesting high temperatures ($T_e \sim 4 \times 10^4$ K), more suggestive of shock heating than photoionization equilibrium. Photoionization models in which the metals are depleted by roughly an order-of-magnitude are computed in an unsuccessful attempt to reproduce these high temperatures. An interpretation in terms of a multicomponent photoionized structure, in which dense regions produce the ultraviolet lines and lower density regions are responsible for the optical lines, is found to be in better agreement with the observations. In this model the inner edge of the narrow-line region is determined by the stability of gas clouds against disruption by radiation pressure. Iron appears to be present in the gas phase in inner regions of the narrow-line region, but may be depleted in outer regions. The O III spectra of other Seyfert galaxies, derived from the literature, suggest that inhomogeneities often affect O III spectra.

Subject headings: galaxies: individual (III Zw 77) — galaxies: Seyfert — line formation — spectrophotometry — ultraviolet: spectra

I. INTRODUCTION

The Seyfert 1 galaxy III Zw 77 has one of the highest ionization emission-line spectra in the Lick Observatory sample (Osterbrock 1981). It is therefore a benchmark in any study relating ionization to other properties of the Seyfert phenomenon, such as continuum shape or luminosity. Despite the fact that this nearby ($z = 0.03374$) galaxy is fairly bright ($m_p \sim 15.4$), it has remained unobserved with the *IUE*. This paper reports nearly simultaneous optical and ultraviolet observations of III Zw 77 and presents a discussion of its emission-line and continuous spectrum.

II. OBSERVATIONS

Vacuum ultraviolet spectral observations with the *International Ultraviolet Explorer* were directed from the Goddard Space Flight Center. Both the large (10″ × 20″) entrance aperture and low resolution ($\delta\lambda \approx 6$ Å shortward of 2000 Å and 8 Å longward) were used. The short-wavelength region (1000 Å–2000 Å) was observed on 1983 August 9–10 (image SWP 20652) with a 450 minute exposure. The long-wavelength region (2000 Å–3100 Å) was observed on 1983 August 10–11 (image LWR 16570) with a 420 minute exposure. Standard reduction procedures (IUESIPS) were used to calibrate the data. The ultraviolet spectrum is shown in Figure 1. Several strong emission lines are present in our spectra; their measured fluxes are given in Table 1.

After the short-wave exposure was read out, it was realized that pixels near the center of the Lyα line had been exposed to levels which are on extrapolated portions of the *IUE* image transfer function. Although not necessarily defective, these data are not especially reliable. A second, shorter exposure spectral image of III Zw 77 was obtained on 1984 March 8 (image SWP 22442, 50 minute exposure). Essentially the same Lyα flux was measured. Optical data obtained at the same time showed that the emission-line fluxes were nearly constant over the 7 months between the two exposures. Only the longer exposure data are used here because of their superior signal-to-noise ratio.

Nearly simultaneous optical observations were made with the Lick Observatory 3 m Shane reflector on 1983 August 12/13 through August 17/18. All the spectral scans were taken with the image-tube image-dissector scanner developed by Robinson and Wampler (1972), and the Cassegrain spectrograph and peripherals developed to match it by Miller, Robinson, and Wampler (1976). Scans were taken with "normal-dispersion" gratings (600 lines per mm), giving a resolution of approximately 10 Å in the ground-based ultraviolet, blue, red, and near-infrared spectral regions, covering (with considerable overlap), the spectral range 3500–8000 Å. Most of these scans were taken with a slit size 2.″7 × 4″ projected on the sky. In addition, however, shorter exposure scans

[1] *Lick Observatory Bulletin* No. 1059.
[2] Guest Observer with the *International Ultraviolet Explorer*.

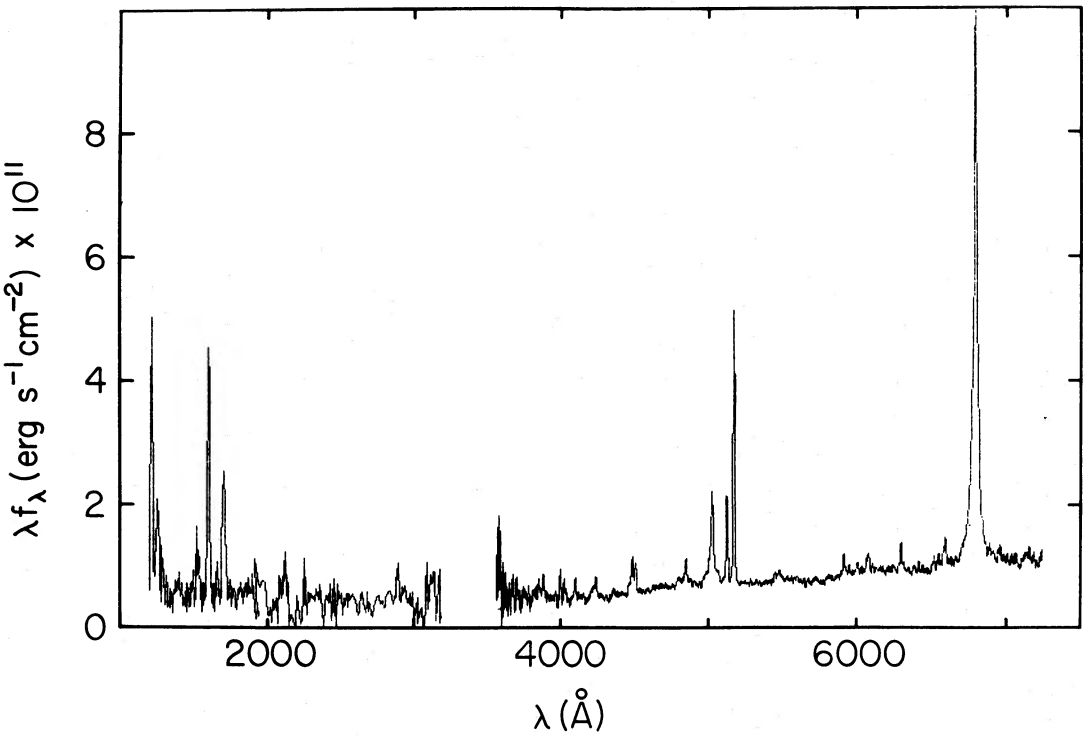

FIG. 1.—The ultraviolet to optical spectrum of III Zw 77. The optical data are the combination of a blue and red scan which overlap in the region near Hβ. The ultraviolet data consist of long- and short-wave scans, which join near 2000 Å. The data are corrected for intrument response, and atmospheric absorption (for the optical data) but are uncorrected for interstellar reddening or the different entrance apertures employed.

were taken with a slit size 8″ × 8″, for the absolute calibration, to minimize the effects of differential seeing and atmospheric dispersion. The standard stars were used for this calibration were BD +28°4211, BD +33°2642, and Hiltner 102 as measured by Stone (1974, 1977).

In addition, scans were taken with a "high-dispersion" grating (1200 lines per mm, giving resolution approximately 5 Å) in the ultraviolet, Hβ, and Hα regions. The total integration times during which III Zw 77 was actually observed totaled 320 minutes with the normal dispersion grating and the 2″.7 × 4″ slit, 160 minutes with the same grating and the 8″ × 8″ slit, and 224 minutes with the high-dispersion grating, all with the 2″.7 × 4″ slit. Considerably less additional integration time was spent on the standard stars, which of course are much brighter than III Zw 77. A composite of several of the observations of III Zw 77 is also shown in Figure 1.

The resulting absolute flux, $F(\mathrm{H}\beta) = 6.5 \pm 0.3 \times 10^{-14}$ ergs cm^{-2} s^{-1} in the rest frame of the Sun, corresponding to $6.9 \pm 0.3 \times 10^{-14}$ ergs cm^{-2} s^{-1} in the rest frame of III Zw 77, is about 30% smaller than the value measured in the earlier paper (Osterbrock 1981). Part of the difference is probably due to variations in the broad-line gas, for the [O III] λ5007/Hβ measured now is about 15% larger than in the previous paper, and the forbidden lines, emitted over a much larger volume, may be assumed constant over the time interval of approximately 4 yr. The remaining difference is no doubt the result of systematic errors in the calibration procedure, but as the present measurements were carried out with a large slot and with significantly more standard-star measurements, they are to be preferred. The true probable error of the Hβ flux, including not only the internal errors quoted above but the systematic effects due to the use of a standard extinction correction, etc., is probably more like $\pm 0.7 \times 10^{-14}$ ergs cm^{-2} s^{-1}. The measured ratios for all these scans were averaged and are presented in Table 1, expressed as absolute fluxes from the measured Hβ fluxes. All fluxes are in the rest frame of III Zw 77, that is, the flux measured in the rest frame of the Sun has been multiplied by $(1 + z)^2$.

No corrections for interstellar reddening have been applied to the data in Figure 1 and the measured intensities in column (3) of Table 1. Burstein and Heiles's (1981) data suggest that reddening due to the Galaxy should be small in the direction of III Zw 77, so our main concern will be for reddening intrinsic to the Seyfert galaxy. Similarly, no corrections for differences in entrance apertures or absolute calibrations have been made. Evidence summarized later suggests that the reddening is small ($E[B-V] \leq 0.2$ mag). The two-dimensional *IUE* PHOTOWRITE shows that the continuum and emission lines come from an unresolved source (<2″), so the fact that the *IUE* entrance aperture is considerably larger than that used in the optical observations should not be a problem. The optical continuum shows only small evidence of starlight. (Osterbrock [1981] finds a contribution from the featureless continuum of $f_{\mathrm{FC}} = 0.85 \pm 0.10$ at 4800 Å, and that the featureless continuum has a power-law [or logarithmic slope] of $\alpha \approx 1.5$.) Apparently both ultraviolet and optical spectral regions mainly sample the unresolved nonthermal featureless continuum source, and no corrections for the different entrance apertures are needed.

III. THE EMISSION LINES

III Zw 77, like all Seyfert 1 galaxies, has an emission-line spectrum which is formed in at least two regions; a lower density narrow-line region, and a higher density broad-line region (this picture is, of course, oversimplified). Judging from the optical spectrum (see Osterbrock 1981), we would expect some of the ultraviolet emission lines to consist of at least two

TABLE 1

EMISSION-LINE FLUXES

Ion (1)	λ (Å) (2)	$I \times 10^{13}$ (ergs cm^{-2} s^{-1}) (3)	I/I(Lyα) $E(B-V) = 0.0$ (4)	I/I(Lyα) $E(B-V) = 0.1$ (5)	I/I(Lyα) Seyfert 2 (6)
Lyαn	1216	8.917	1000.	1000.	1000.
Lyαb	1216	<2.7	<300.	<300.	
N v	1240	0.5:	60.:	59.:	
?	1472	0.6:	70.:	60.:	
N IV]	1486	0.5	60.	51.	
C IVn	1549	3·8	430.	360.	220.
C IVb	1549	<3.0	<340.	<285.	
He II	1640n	0.8	90.	74.	
?	1650:	1.4	157.	129.	
O III]	1663	0.7	79.	65.	
C III]	1909	0.5:	56.	48.	100.
[O III]	2322	<0.2	<23.	<21.	
Mg II	2798	0.3:	34.:	24.:	33.
—	3409	0.013	1.4	0.88	
[Ne V]	3426	0.20	23.	14.	22.
O III	3444	0.023	2.6	1.6	
[Fe VII]	3588	0.042	4.7	3.0	
[O II]	3727	0.077	8.6	5.3	58.
[Fe VII]	3760	0·066	7.4	4.5	
[Ne III]	3869	0.12	13.	7.9	25.
[Fe V]	3893	0.056	6.3	3.8	
—	3913.8	0.016	1.8	1.1	
[Ne III] + Hε	3968	0.068	7.6	4.6	
[Fe V]	4071	0.038	4.3	2.6	
—	4088	0.029	3.2	1.9	
Hδ	4102	0.096	10.8	6.4	
—	4317	0.032	3.6	2.1	
Hγ	4340	0.024	2.7	1.6	
[O III]	4363	0.092	10.3	6.0	3.8
He II	4686n	0.091	10.2	5.8	5.3
He II	4686b	0.15	17.	9.7	
Hβ	4861c	0.69	77.	43.	18.
[O III]	4959	0.30	33.6	18.7	65.
[O III]	5007	0.86	96.	54.	196.
[Fe XIV] +	5305	0.059	6.3	3.4	
[Fe VII]	5721	0.047	5.3	2.8	
He I	5876n	0.074	8.3	4.4	
[Fe VII]	6087	0.069	7.7	4.0	1.8
[O I]	6300	0.030	3.4	1.8	10.4
[S III]	6312	0.006	0.7	0.4	
[Fe X]	6375	0.072	8.1	4.2	0.7
[N II]	6548	0.057	6.4	3.3	18.
Hα	6563c	3.20	359.	185.	56.
[N II]	6583	0.17	19.	9.8	53.
[S II]	6717	0.022	2.5	1.3	13.
[S II]	6731	0.027	3.0	1.5	13.
—	7043	0.021	2.4	1.2	
He I	7065	0.032	3.6	1.8	
[O II]	7320	0.016	1.8	0.90	
[O II]	7330	0.008	0.9	0.5	
[Fe XI]	7893	0.020	2.2	1.1	

NOTE.—"b" indicates a broad component; "n" indicates a narrow component; "c" indicates that the line is composite and the measured flux refers to the entire broad plus narrow profile.

components: a sharp component of width $\sim$100–500 km s^{-1}, superposed upon a broad base extending perhaps to a full width at zero intensity (FWZI) of $\sim$11,000 km s^{-1}. Since the spectral resolution of the *IUE* corresponds to a velocity resolution of only $\sim$1200 km s^{-1} for most ultraviolet lines, we would expect to observe unresolved sharp central components superposed upon a broad base (perhaps with fairly small residual intensity) if both components are present.

Figure 2 shows line profiles for some of the stronger ultraviolet and optical emission lines in our simultaneous spectra. The [O III] λ5007 line is an example of a line with only the narrow component, while Hβ has contributions from both narrow and broad components. It is not possible to make similar statements concerning the ultraviolet data, since our signal-to-noise ratio is relatively poor in the continuum, and any broad base could well go undetected. (If the conventional picture of two emission-line regions, an inner, dense, broad-line region and an outer, more tenuous narrow-line region, as described, for instance, by Davidson and Netzer [1979], applies to III Zw 77, we would expect both broad and narrow contributions to the two ultraviolet lines shown.) It is possible

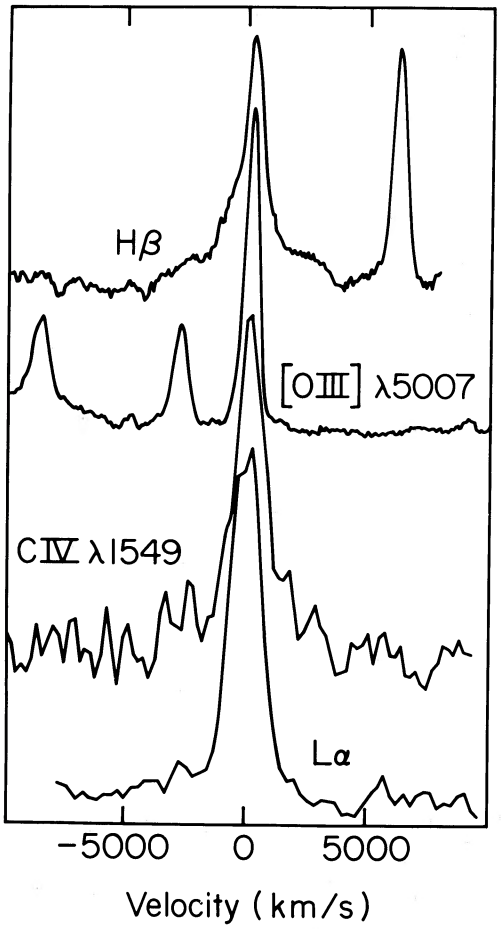

FIG. 2.—Emission-line profiles. The emission lines of of III Zw 77 contain contributions from both broad and narrow components. This figure compares profiles of several of the stronger emission lines in our data. The Hβ line is a combination of broad and narrow components, while the [O III] 5007 line is considerably sharper. *IUE* observations of C IV λ1549 and Lyα do not have the high signal-to-noise ratio or spectral resolution of the optical data, so it is difficult to determine whether broad bases are present in them too.

that both Lyα and C IV λ1549 do have broad bases, although the main contributor to both lines (and the only one measured) appears to be narrow. Detections of other (weaker) ultraviolet emission lines have sufficient signal-to-noise ratio to measure only the sharp core; this presents a problem when comparing ultaviolet and (higher signal-to-noise ratio) optical data. All the ultraviolet line intensities in Table 1 refer to the sharp, easily measured, cores only. The majority of the optical lines are also narrow, with a few exceptions such as a possible component of He II λ4686 (denoted by the "b" after the wavelength) and the Balmer lines. In this respect, the spectrum listed in Table 1 is similar to that of a Seyfert 2 galaxy, except for the broad components. Upper limits to the broad component of Lyα and C IV λ1549 have been set by setting a continuum as low as possible, using Hβ as a template, and putting the broad component as high as possible.

The feature at λ1650 (Fig. 3; the wavelength scale has been corrected for a redshift of $z = 0.03374$) is a blend of at least three lines. One component is He II λ1640, and the O III] $\lambda\lambda$1661, 1666 doublet is identified as the contributor to the longward portion of the feature. (In some portions of this paper we will denote both components of the doublet as λ1663.) Intensities of the contributors to the blend are estimated by fitting C IV λ1549 profiles, shifted to the appropriate wavelengths, to the individual components. The $\lambda\lambda$1661/1666 doublet intensity ratio is assumed to be $0.41 = 1/2.45$, the value calculated from the known transition probabilities (Nussbaumer and Storey 1981). Figure 3 shows the estimated contributions from these lines. Clearly, there is an important, third contribution to the blend, centered about 1650 Å. We have not been able to identify it. Inspection of the camera image does not reveal cosmic-ray hits, and "hot" pixels are not known to occur at the position of this blend ($\lambda \approx 1706$ Å; Hackney, Hackney, and Kondo 1984).[3]

The He II spectrum suggests that the intrinsic reddening is small. Osterbrock (1981) notes that the He II λ4686 profile shows two components, one quite broad and blueshifted relative to the narrow component. Judging from the small residual intensity of the broad component of λ4686, and the modest signal-to-noise ratio of the ultraviolet data, we would not expect to be able to detect the broad component of He II λ1640, even if it is present. In fact, the line deconvolution shown in Figure 3 reveals only narrow λ1640. The observed value of the He II $\lambda\lambda$1640/4686 ratio (comparing the narrow component of λ4686, and the intensity of λ1640 estimated here) is $\sim$8.8, in the neighborhood of the theoretical recombination case B ratio of 5.6–7.6 (Seaton 1978). More recent transfer calculations (cf. MacAlpine 1981; MacAlpine *et al.* 1985; Eastman and MacAlpine 1985; Netzer, Elitzur, and Ferland 1985) suggest that values of $\sim$7–10 can be obtained in some clouds. Our measured value, although uncertain, is consistent with these calculations if there is little or no reddening ($E[B-V] < 0.1$ mag).

The hydrogen-line spectrum provides another limit to the reddening. The observed value of the Lyα/Hβ ratio is 13, with no correction for reddening. This ratio cannot be compared directly with theory because the two lines are not formed in the

[3] Although we have not been able to identify two of the ultraviolet lines, we have found a plausible identification for the line at λ7613.1 Å noted by Osterbrock (1981). We believe it to be the $2s^2 2p\,^2P_{1/2}$–$^2P_{3/2}$ transition of [S XII], with an air wavelength of 7611.0 Å $\pm$ 0.4 Å (Edlén 1969). This identification is in keeping with the levels of ionization indicated by other coronal lines, such as Fe XIV λ5304.

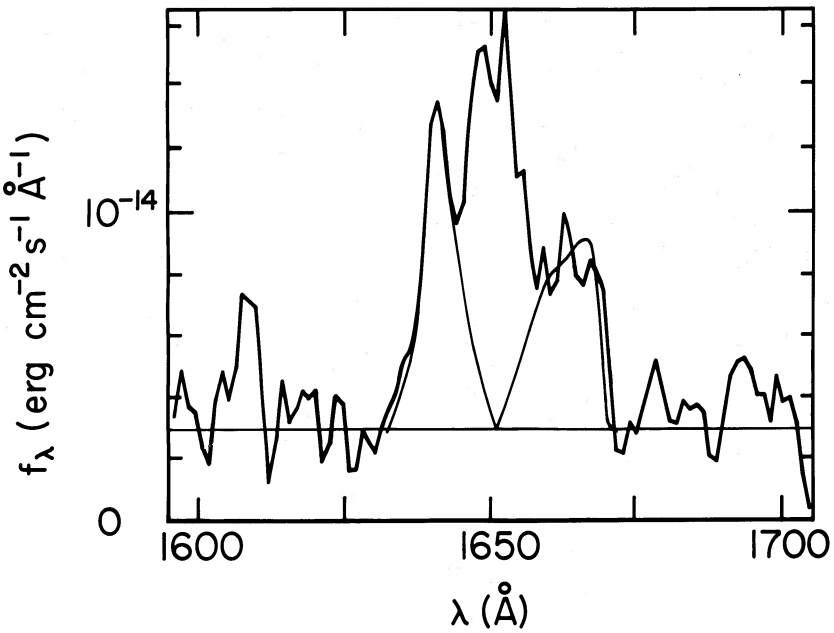

FIG. 3.—The λ1650 blend. This feature contains at least three contributors, He II λ1640, O III] λ1663, and an unidentified line with a wavelength near 1650 Å. A deconvolution into contributions from He II and O III] is shown, assuming line profiles similar to C IV.

same region (the Lyα measurement refers to only the sharp component, while the higher signal-to-noise Hβ measurement includes both broad and narrow components). The ratio is close to that predicted by photoionization models of the broad-line region (Kwan and Krolik 1981), although we expect both lines to have contributions from lower density regions. Low-density gas can have ratios of Lyα/Hβ larger than calculated in case B because of collisional excitation of Lyα. Values as large as Lyα/H$\alpha \sim 50$ are predicted (Pequignot 1984), and Lyα/H$\beta \approx 55 \pm 20$ is inferrred (Ferland and Osterbrock 1986) in Seyfert 2 galaxies (where the Hβ line is not contaminated with a broad component). If we take 55 as the largest likely value of the ratio, the upper limit to the color excess is $E(B-V) < 0.25$ mag.

The O III spectrum suggests high temperatures. The combined ultraviolet and optical data include five lines from three excited terms of O III; $\lambda\lambda$5007, 4959, 4363, and the $\lambda\lambda$1661, 1666 doublet. The $\lambda\lambda$4363/5007 intensity ratio lies between 0.11 and 0.13 (for a range in reddening of $0 < E[B-V] < 0.3$ mag), while the $\lambda\lambda(1661+1666)/5007$ ratio lies between 0.8 and 2.6 for the same reddening range. (Additional uncertainties are present because of the signal-to-noise ratio in the ultraviolet data, and because of the need for a line deconvolution.) Figure 4 shows the electron density (N_e)–temperture (T_e) plane, with regions that can reproduce the indicated line ratios. (The regions are bands because of the range of line ratios allowed by the uncertainty in the reddening; they correspond to a range of $0 < E[B-V] < 0.3$.) This figure is the result of a six-level atom calculation, using atomic data summarized by Mendoza (1983), and assuming that the level populations are determined by the balance between collisional and radiative processes. Effects of recombination (radiative or dielectronic), charge transfer, and photoionization are not included.

Taken at face value, the measured intensities suggest temperatures near those normally associated with shock heating, where T_e can be as high as $\sim 10^5$ K in the O^{+2} region. No set of physical conditions can reproduce the line ratios if they are corrected for a reddening larger than $E(B-V) = 0.2$ mag; if little or no reddening correction is applied then we find a band of permitted values extending between roughly ($N_e \approx 10^4$ cm^{-3}; $T_e \approx 10^5$ K) and ($N_e \approx 3 \times 10^5$ cm^{-3}; $T_e \approx 4 \times 10^4$ K).

We do not think that the strong $\lambda\lambda$1661, 1666 lines are spurious; "hot" pixels do not occur at the Earth-frame position of the line (1719 Å; Hackney, Hackney, and Kondo 1984), and the PHOTOWRITE shows no evidence of a cosmic-ray hit. The feature has a width perpendicular to the dispersion which is similar to the neighboring continuum. A possibility is that the unidentified line near λ1650 is actually a doublet, with a component beneath the O III] lines. This seems unlikely since other Seyfert galaxies have similar O III spectra (discussed in the Appendix) but do not show the λ1650 feature. Another possibility is that more than one region contributes to the formation of the O III spectrum. A dense photoionized region would mainly emit the ultraviolet semiforbidden O III] lines, while low-density regions would emit the forbidden [O III] lines. It is also possible that our assumptions concerning the processes affecting the level populations of the O^{+2} ion are incorrect, or that the atomic data are badly in error. The latter does not seem to be likely as the O III spectra of planetary nebulae can be reproduced by models (Harrington *et al.* 1982).

The suggestion of high temperatures in the O III zone raises fundamental questions about the nature of the emitting gas in III Zw 77; could it be shock heated? In general, the temperatures deduced from the optical emission-line spectrum are also high; Osterbrock (1981) finds that the [Fe VII] lines indicate temperatures between 2 and 5×10^4 K, but points out that this is too low for shock heating to be important for Fe^{+6}. One way to address this question is by a direct comparison between the emission-line spectrum of this object, with the spectrum of a class of objects which are believed to be photoionized, the Seyfert 2 galaxies. This is a more meaningful comparison than with broad-line objects because most of the fluxes in Table 1 refer only to the narrow core of the emission lines, either because only the sharp cores are detected (in the

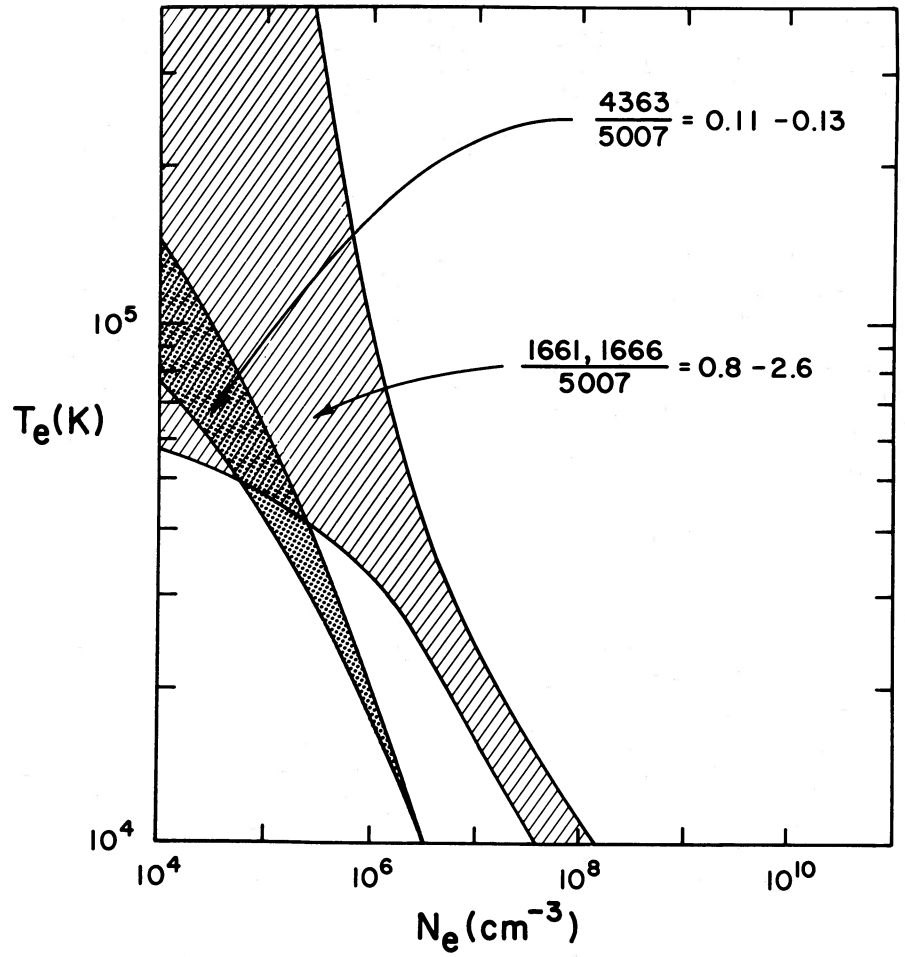

FIG. 4.—The O III spectrum. This figure shows the ranges of permitted physical conditions, allowed by the observed O III line ratios. Predicted intensities are the result of a calculation including the lowest six levels of O III, through $2p^3\,{}^5S_2$. The two bands correspond to observed values of the [O III] $\lambda\lambda$4363/5007 and O III] $\lambda\lambda$1663/[O III] 5007 ratios. The bands include uncertainties due to reddening as large as $E(B-V) = 0.3$ mag, and described by a galactic interstellar reddening law.

case of the ultraviolet lines), or because only sharp components are believed to be present (the optical forbidden lines). (The notable lines in Table 1 which have significant contributions from their broad components are the Balmer lines, and those indicated by a "b" after the wavelength.)

The mean composite emission-line spectrum of the sample of Seyfert 2 galaxies studied by Ferland and Osterbrock (1986) is given in the last column of Table 1. This composite spectrum has been corrected for reddening, as described in the reference. The discussion above suggests that the line reddening in III Zw 77 is small ($E[B-V] \leq 0.1$ mag), but even this amount of reddening will affect the ultraviolet to optical spectrum. Column (5) of the table gives the spectrum of III Zw 77 after correcting for a reddening of $E(B-V) = 0.1$ (assuming the interstellar reddening curves given by Seaton [1979]); this gives an idea of the dispersion in the line ratios produced by the permitted range in reddening. The composite Seyfert 2 spectrum has a large dispersion (caused by a real difference between line spectra of different objects) which typically amounts to a factor of 2 relative to Lyα.

Although the spectra are generally similar, several major differences exist. The Lyα/Hβ ratio in III Zw 77 is much smaller than in Seyfert 2 galaxies because of the broad-line region contribution to Hβ in the Seyfert 1 galaxy. Forbidden lines are generally weaker (relative to the narrow Lyα) in III Zw 77 than in Seyfert 2 galaxies, and this is especially true of lines formed by ions of low-ionization potential (e.g., lines of [S II], [N II], [O II], and [O I] are weak). This is probably an ionization difference rather than density difference, because [O I] lines have a relatively high critical density, but yet are weak in III Zw 77 (see also De Robertis and Osterbrock 1986). Although the [O III] $\lambda\lambda$5007, 4959 lines are weaker in III Zw 77 than in Seyfert 2 galaxies, lines from more highly excited levels of O^{+2} (λ4363 and the $\lambda\lambda$1661, 1666 doublet) are stronger relative to Lyα. This suggests that the O III line-forming region is hotter in III Zw 77. Lines of high stages of ionization of Fe are much stronger in III Zw 77, a fact which first drew attention to this object (Osterbrock 1981). These clues suggest that the gas in the emission-line regions of III Zw 77 might be both hotter and more highly ionized than is found in Seyfert 2 galaxies.

A strong suggestion that the gas in III Zw 77 is photoionized comes from the equivalent widths of the emission lines; these are similar to other active nuclei. Yee (1980) and Shuder (1981) studied line-continuum correlations for a large sample of active nuclei. They found a one-to-one correlation between the Hα luminosity and the luminosity in the featureless continuum at 4800 Å, L(NT 48). The fact that this correlation was found over

a range of nearly 6 orders of magnitude in luminosity was a strong suggestion that photoionization was the dominant energy source in the class of active nuclei. The same parameters for III Zw 77 (L[Hα] = 8.8×10^{41} ergs s^{-1} cm^{-2} and L[NT 48] = 2.1×10^{28} ergs s^{-1} cm^{-2} Hz^{-1} for an assumed distance of 135 Mpc, deduced from the redshift and $H_0 = 75$ km s^{-1} Mpc^{-1}, as assumed by Shuder in his paper) place it near the center of Shuder's correlation. Similarly, it is possible to compare the equivalent width of Lyα (W_λ[Lyα] = 180 Å) with the sample of high-redshift quasars and low-redshift Seyfert galaxies studied by Wu, Boggess, and Gull (1983). Again III Zw 77 is not too far from the mean. These ratios of line-to-continuum suggest that the physics governing line formation in III Zw 77 is not too different from that occurring in the "average" active galactic nucelus (AGN). This, in turn, suggests that photoionization rather than shock heating is the energy source in the emission-line regions of III Zw 77. Other evidence against the importance of shock heating in III Zw 77 is summarized by Osterbrock (1981). We will assume that III Zw 77 is an extreme case of the active galaxy phenomenon (in terms of level of ionization) and will interpret its spectrum in these terms.

IV. THE CONTINUUM

Questions conerning the nature and form of the featureless continuum in active nuclei are both fundamental and difficult to address (see, for example, the reviews by Elvis and Lawrence [1985], and Stein and O'Dell [1985]). In this section we combine some observed properties of III Zw 77 with general features of other active nuclei to estimate the form of the ionizing continuum in this object. Intensities of various emission lines will be used to infer properties of the far-ultraviolet continuum; we assume that the gas is photoionized, and not shock heated, throughout this section.

Before continuing, we summarize some general features of AGN continua. It has long been known that the optical continuum of AGN is roughly approximated as a power law extending far into the ultraviolet, and that the exponent has a value near unity (that is, $f_\nu \propto \nu^{-1}$). More recently, a great deal of attention has been focused on the effects of the pseudocontinuum formed by the mixture of Fe II and Balmer emission (see, for example, Wills, Netzer, and Wills 1985; Oke, Shields, and Korycansky 1984). We note here that III Zw 77 is not a strong emitter of either permitted or forbidden Fe II. These studies, and energy budget arguments such as Netzer (1985), suggest that the far-ultraviolet continuum may actually be very flat ($f_\nu \propto \nu^{-0.5}$) in typical nuclei. Whatever the case, the observed ratio of ultraviolet to X-ray continuum fluxes demands that the continuum roll over sharply between the satellite-ultraviolet continuum (near 10 eV) and the soft X-ray ($h\nu > 500$ eV), as the mean exponent between the ultraviolet and soft X-ray is ~ 1.4 (Zamorani *et al.* 1981). Studies in the X-ray band show that the spectrum between 0.5 keV and 10 keV is generally described by a power law with exponent 0.7 and little or no absorption (Mushotzky 1982; Reichert *et al.* 1985), although exceptions are often found. Most recently, evidence for an excess of $h\nu < 0.5$ keV X-ray flux above this power law has been found (Elvis 1986; Arnaud *et al.* 1985); an interpretation is that this is the high-energy tail of a thermal source associated with the flat ultraviolet continuum component, as suggested by Malkan and Sargent (1982).

Figure 5 shows mean optical and ultraviolet continuum

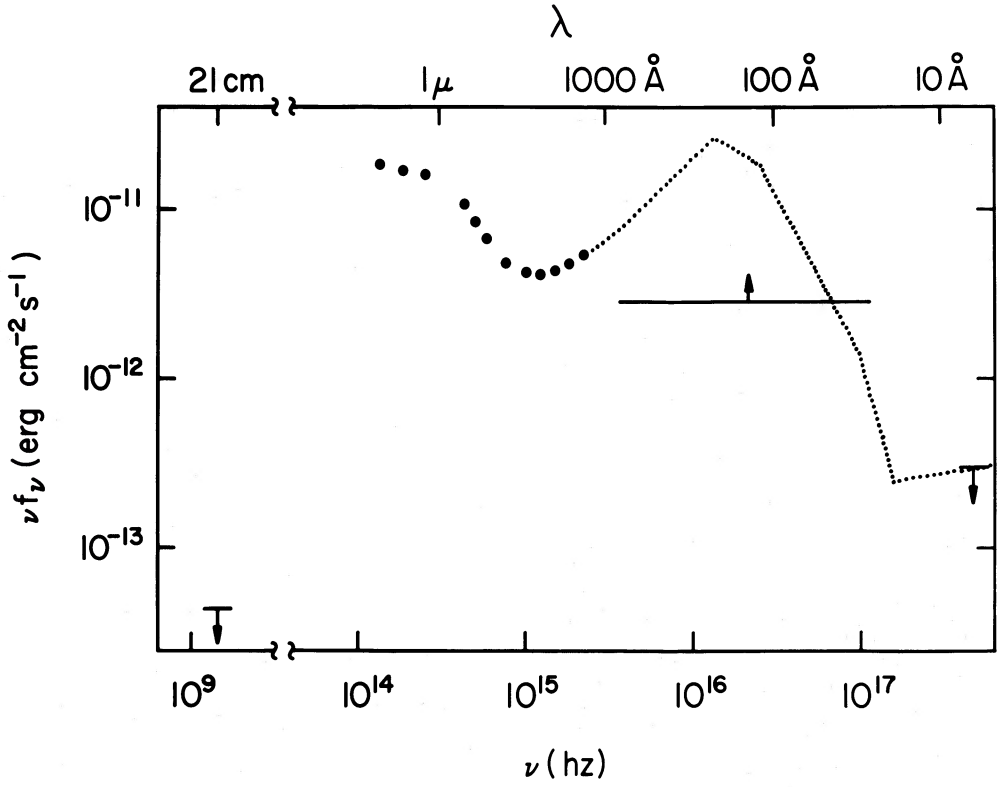

FIG. 5.—Continuous energy distribution of III Zw 77. The data are taken from a variety of sources, as mentioned in the text. The solid line indicating the lower limit to the flux shortward of 912 Å is the sum of the total intensities of all observed emission lines. No corrections for interstellar reddening, entrance aperture, variability, or different absolute calibrations have been made. The dotted line in the unobservable extreme ultraviolet is the continuum used in the photoionization calculations and was deduced from a consideration of the helium spectrum and the power in ionizing radiation needed to sustain the emission-line region.

fluxes for III Zw 77, obtained by averaging over ~75–100 Å intervals chosen to be free of emission lines. III Zw 77 has been detected, or upper limits set, across much of the electromagnetic spectrum. The infrared continuum was measured by Balzano and Weedman (1981), and upper limits to the 21 cm radio flux were set by Wilson and Meurs (1982). Dressel and Wilson (1985) set an upper limit (3 σ) of $\nu f_\nu < 3 \times 10^{-13}$ ergs cm^{-2} s^{-1} in the *Einstein* IPC soft X-ray band. It is important to remember that these observations were not simultaneous with ours, and that over 50% of the Seyfert galaxies studied vary over time scales of a year or so (Peterson, Crenshaw, and Meyers 1985). Nonetheless, variations are typically small enough that comparisons between optical, radio, infrared, and X-ray observations should be informative. These detections and limits are shown in Figure 5.

The 3 σ X-ray upper limit is consistent with a "conventional" Seyfert galaxy continuum; it corresponds to a value of α_{ox} (the spectral index describing the continuum between 2500 Å and 2 keV; i.e., $f_\nu \propto \nu^{-\alpha}$ox) of $\alpha_{ox} > 1.45$. For comparison, Zamorani *et al.* (1981) report that the average vslue of α_{ox} for radio-quiet objects is 1.46 (+0.05, −0.07). It would be very surprising if III Zw 77 were not a conventional X-ray source, as the [Fe XIV] λ5303 emission line is present, a direct indication that the continuum has significant flux at and just above its ionization potential of ~0.4 keV. (This, of course, is not significant if the highly ionized gas is not photoionized.)

The emission-line spectrum discussed above suggests that the reddening of III Zw 77 is small. The optical-ultraviolet continuum also suggests that there is only slight extinction. Malkan (1984) lists optical/ultraviolet flux ratios for a large sample of active nuclei. He finds mean ratios of

$$\frac{f_\nu(4220)}{f_\nu(1770)} = 1.55 \text{ and } \frac{f_\nu(4220)}{f_\nu(1465)} = 1.80 .$$

For comparison, the same ratios in III Zw 77, after correcting for starlight contamination, are both ~3.3. If the featureless continuum of III Zw 77 is close to Malkan's deduced AGN continuum (a proposition certainly open to question), the reddening to the continuum source is $E[B-V] \approx 0.1$ mag. Unfortunately the scatter is large in the region of Malkan's diagram where III Zw 77 lies (log $[L_{4220}] = 28.5$ ergs s^{-1} Hz^{-1}), so this too is only a suggestion of small reddening.

If the gas is photoionized, a simple argument can be used to estimate the power in the extreme ultraviolet continuum ($\lambda < 912$ Å). If the emission-line regions are photoionized by the extrapolated featureless continuum, we can set a lower limit to the extreme ultraviolet continuum by simply adding the fluxes of all the emission lines detected in the ultraviolet and optical data. (Note that this sum includes recombination lines, such as Lyα, and hence is equal to the total energy of the ionizing radiation absorbed, and not just the kinetic energy of the photoelectrons; see, for example, Osterbrock 1974.) The sum of the total energy in emission lines in the rest frame of III Zw 77 comes to 2.5×10^{-12} ergs cm^{-2} s^{-1} and is a lower limit to the absorbed energy because the covering factor and optical depth of the emitting gas in the ionizing continuum are unknown, some coolants and recombination lines are unobservable and because no correction for interstellar reddening has been applied. The largest of these uncertainties is the covering factor; if a typical value of 10% is assumed the continuum is raised by a factor of 10. This limit should not, however, be affected by line transfer and collisional effects, such as those described by Kwan and Krolik (1981), as long as these processes simply shift cooling from one emission line to another. The lower limit to the energy in the ionizing continuum is shown in Figure 5; it suggests that the rise in the continuum seen in the *IUE* spectra shortward of 1500 Å continues well beyond 1 Ry. That AGN continua in general must rise beyond the Lyman limit has been suggested by MacAlpine *et al.* (1985) and Netzer (1985).

Similarly, the He II spectrum offers an indicator of the radiation field beyond 4 Ry (see also MacAlpine 1981). In photoionization equilibrium, the ratio of the intensity of a He II recombination line, such as λ4686 or λ1640, to the intensity of a hydrogen recombination line such as Hβ or Lyα, is given by the ratio of the number of ionizing photons in the helium and hydrogen ionizing continua, i.e.,

$$\frac{Q(\mathrm{He}^{+2})}{Q(\mathrm{H}^{+})} = \frac{\int_4^\infty [f_\nu(\nu)/h\nu]d\nu}{\int_1^\infty [f_\nu(\nu)/h\nu]d\nu} ,$$

providing an estimate of the far-ultraviolet continuum which is independent of the covering factor. This assumes that the emitting gas is optically thick to the majority of the photons with $h\nu \geq 1$ ryd, neglects heavy element opacities, and assumes that each He^+ ionization produces a recombination line which then ionizes hydrogen. These assumptions are in general (~25%) agreement with the numerical calculations discussed below. (Some He^+ ionizing radiation is absorbed by heavy elements.)

A strong feature is present near the wavelength of He II λ4686, but its strength, breadth, and blueshift relative to the other emission lines makes its interpretation unclear (Osterbrock 1981). The ultraviolet spectrum shows λ1640, and its strength relative to Lyα can be readily measured. Both λ1640 and Lyα are unresolved in our *IUE* spectra, so the gas emitting the ultraviolet lines is likely to be the lower density, small line-width component, identified as the narrow-line region in the optical spectra. For conditions appropriate to such gas the He II line should have an emissivity close to case B predictions, while Lyα may be strengthened somewhat (<50%) by collisional effects. In this case the observed λ1640/Lyα ratio of ~0.09 can be related to the continuum near an energy of 4 Ry by

$$\frac{Q(\mathrm{He}^{+2})}{Q(\mathrm{H}^{+})} = \frac{I(\lambda 1640)}{I(\mathrm{Ly}\alpha)} \frac{4\pi j(\mathrm{Ly}\alpha)}{4\pi j(\lambda 1640)} = 0.041 .$$

This suggests that the continuum begins to roll over at energies only slightly above 4 Ry.

Figure 5 shows a possible extreme ultraviolet continuum, based on estimates of the total power in the ionizing continuum, the He II spectrum, and the fact that the continuum must turn down before it reaches the *Einstein* IPC band (this last constraint if valid only in a statistical sense, because the X-ray continuum in III Zw 77 has not actually been detected). The large "bump" near ~500 Å is quite similar to features deduced for quasars and other Seyfert galaxies (Elvis 1986).

V. MODEL CALCULATIONS

a) Goals and Constraints

Can the observed spectrum of III Zw 77 be fitted with a photoionization model? This question is important because, although the high levels of ionization observed in its spectrum distinguish III Zw 77 among the Seyfert galaxies, its hydrogen-line equivalent widths (relative to the featureless continuum) are fairly typical. There is a well-established correlation

between emission-line luminosity and the power in the optical featureless continuum (Shuder 1981). This is convincing evidence that the class of active nuclei is photoionized by the underlying continuum. The fact that III Zw 77 obeys Shuder's correlation strongly suggests that the basic physics governing line formation in this object must be similar to other active galaxies. Composite shock-heated–photoionization models have been proposed for active nuclei (see Contini and Aldrovandi 1983); here we will assume that photoionization is the sole energy input to the emitting gas. Although it is naive to expect simplified models to fully reproduce the spectrum produced in as complicated an environment as an active galaxy, we can examine the global thermal properties of model nebulae to check whether it is possible to reproduce the observed O III spectrum with its remarkable consequences.

Calculations are performed with the photoionization program most recently described by Ferland and Osterbrock (1986). We first describe some physical processes which are included, but which are not normally important in galactic nebulae. We are especially interested in processes which could affect the [O III] emission lines, $\lambda\lambda$1661, 1666, 4363, and 5007, which we use as diagonostic indicators of the physical conditions. The goal is to determine whether nontraditional processes might affect the emission lines used to deduce the surprisingly high temperatures.

Charge transfer of O^{+3} with H^0 is known to preferentially populate singlet and triplet states of O^{+2} (Dalgarno and Sternberg 1982; see also Osterbrock, Dahari, and Ekberg 1983) and has been included with the rate coefficients given in these references. Radiative recombination with ground-state ($^2P^o$) O^{+3} can populate either singlet or triplet O^{+2} (but not the quintets, which produce the $\lambda\lambda$1661, 1666 doublet). It has been included as a population mechanism for ^1D and ^1P with the rate coefficients given by Burgess and Seaton (1960). Dielectronic recombination through low-lying autoionizing levels can also populate the ^5S level producing the $\lambda\lambda$1661, 1666 lines and is included with a rate coefficient set to the upper limit quoted by Nussbaumer and Storey (1984). In the models described below, dielectronic recombination is by far the most important of these three processes in changing the O III spectrum.

Photoionization from both inner and valence shells can affect the [O III] spectrum (see, for example, Aldrovandi and Gruenwald 1985; Ferland and Shields 1978). Photoionization from the ^1D level can decrease the O^{+2} abundance in the He^+ zone of nebulae with high-ionization parameters, because the ionization potential of this level is less than the 4 Ry ionization potential of He^+. The ground term of O^{+2} is well-shielded from ionizing radiation by the He^+ opacity, unlike the excited levels. Photoionization affects the relative populations of the levels producing the [O III] spectrum and is especially important as an O^{+2} ionization mechanism.

Inner shell photoionization can also be important. The ground term of O^+ is $2s^22p^3\,^3P$. Removal of one of the $2s^2$ electrons by photons with energies between 42.6 eV and 50.0 eV leave the daughter in the $2s2p^3\,^5S$ term, which gives rise to the $\lambda\lambda$1661, 1666 doublet. Above this energy other terms in the $2s2p^3$ configuration are accessible, and we assume that they are populated according to their statistical weight. Cross sections from Weisheit and Collins (1976) are used. Finally, removal of one of the $1s^2$ electrons of atomic oxygen produces O^{+2} (following Auger ejection) in the $2s2p^3\,^1D$ excited term 27% of the time (McGuire 1969). All of these processes have been included in the following calculations, while the first is by far the most important.

The ionizing continuum is approximated as a set of piecewise continuous power laws, that is,

$$f_\nu = a\nu^{-\alpha},$$

where the spectral index α is given the values

$$\alpha = \begin{cases} 1.23;\ 0.0001\ \text{Ry} < \nu < 0.1014\ \text{Ry} \\ 1.68;\ 0.1014\ \text{Ry} \le \nu < 0.228\ \text{Ry} \\ 1.463;\ 0.228\ \text{Ry} \le \nu < 0.304\ \text{Ry} \\ 0.7223;\ 0.304\ \text{Ry} \le \nu < 0.701\ \text{Ry} \\ 0.1966;\ 0.701\ \text{Ry} \le \nu < 1.21\ \text{Ry} \\ 0.0;\ 1.21\ \text{Ry} \le \nu < 4.01\ \text{Ry} \\ 1.607;\ 4.01\ \text{Ry} \le \nu < 7.64\ \text{Ry} \\ 2.833;\ 7.64\ \text{Ry} \le \nu < 30.40\ \text{Ry} \\ 4.750;\ 30.40\ \text{Ry} \le \nu < 48.18\ \text{Ry} \\ 0.700;\ 48.18\ \text{Ry} \le \nu < 8100\ \text{Ry}, \end{cases}$$

where the frequency is expressed in rydbergs. This matches the observed continuum exactly, and at ionizing energies, has the general properties deduced in § IV. This assumed continuum is illustrated in Figure 5. It is normalized to produce a flux density at 1 Ry of $F_\nu = 9.50 \times 10^{27}$ ergs s^{-1} Hz^{-1}. The luminosity of this continuum integrated over the range 10^{-4}–8000 Ry is 2.1×10^{44} ergs s^{-1}.

b) *One-Component Models*

The aim here is to see whether a simple one-component model, such as that considered by Ferland and Osterbrock (1986), can reproduce the spectrum of III Zw 77. Taken at face value, the emission lines of O^{+2} suggest that the emitting gas is extraordinarily hot by the standards of photoionized nebulae. In the low-density limit, the observed (λ1661 + λ1666)/λ5007 line ratio indicates a temperature near 10^5 K, although temperatures as low as 4×10^4 K can be fitted to the spectrum if the electron density is high enough to deactivate partially the $\lambda\lambda$5007, 4959 lines ($N_e \sim 10^5$ cm^{-3}). For comparison, the temperature characterizing the O^{+2} zone of galactic photoionized nebulae is usually not far from 10^4 K. In this section we investigate just how hot a photoionized gas can be.

If the physical conditions deduced from the O III spectrum are correct, the heavy element abundances of the emitting clouds must be much smaller than solar, and the ionizing continuum energizing the clouds must be very energetic. High temperature is achieved in photoionization equilibrium only if there is a paucity of coolants, as would be the case if the heavy elements had subsolar abundances. A rough indication of how low this composition must be can be made by comparing the intensities of [O III] $\lambda\lambda$5007, 4959 and He I λ5876 observed in III Zw 77. If we assume that the He I line is formed by recombination, and the [O III] lines by collisional excitation, the observed line ratio is related to the ionic abundance ratio by

$$\frac{I(\lambda5007 + \lambda4959)}{I(\lambda5876)} = 24 = \frac{4\pi j(\lambda5007 + \lambda4959)}{4\pi j(\lambda5876)} \frac{N(O^{+2})}{N(He^+)},$$

where the j's stand for the emission coefficients per unit electron and ion density. The result is $N(O^{+2})$/

$N(He^+) = 2.8 \times 10^{-5}$ (± 0.3 dex), where the uncertainty is due only to the variation in emissivities over the range in permitted physical conditions (from $T = 10^5$ K, N_e small, to $T = 4 \times 10^4$ K, $N_e = 10^5$ cm^{-3}). If the O^{+2} and He^+ zones coincide (a good approximation for galactic nebulae, but questionable here, since the He I and [O III] lines do not have the same width), oxygen is depleted by a factor of ~ 300 below the solar O/He abundance ratio of 8.3×10^{-3} (Lambert 1978).

We have computed a model very similar to the one considered by Ferland and Osterbrock (1986) in their study of Seyfert 2 galaxies. The density is inversely proportional to the radius, and the material is assumed to be distributed in optically thin clumps, with a filling factor which is adjusted to produce the observed [O III]/[O II] ratios. The inner radius is chosen to produce very high levels of ionization; in the present model an inner density and radius of $N_H = 10^8$ cm^{-3} and log (r[cm]) = 16.5 were chosen, and the dominant stage of ionization of iron was Fe^{+19}. All elements other than helium were depleted by a factor of 10 relative to hydrogen, and a filling factor of log (ϵ) = -4.2 was chosen. The model is matter bounded; radial integrations stop when [O I] λ6300 reaches an intensity of 3% of [O III] λ5007. This is the simplest model capable of simultaneously matching the high and low ionization lines, as well as the red [S II] doublet (which indicates $N_e \sim 10^3$ cm^{-3} in the region in which it is emitted) and the O III spectrum, which requires higher densities for nebular temperatures.

Table 2 lists some of the predictions of the model. It does come close to matching the observed intensity ratio [O III] λ5007/Lyα, but does not reproduce C III], C IV, or O III] λ1663. Although the detailed physical processes mentioned above did alter the O III spectrum to some extent, their cumulative effects were not large enough to invalidate the use of the $\lambda\lambda$1663, 4363, 5007 lines as thermometers. We have tried very hard to find models in which the electron temperatures in the O^{+2} zone were as high as possible; mean O^{+2} zone temperatures above 2×10^4 K were seldom found in any model, and the temperature in the listed model ($\sim$18,000 K) was more typical.

TABLE 2

PREDICTED INTENSITIES–ONE-COMPONENT MODEL

Ion	λ (Å)	I/I(Lyα)
Lyα	1216	1000.
N V	1240	4.1
C VI	1549	56.7
He II	1640n	49.3
O III]	1663	6.9
C III]	1909	43.9
Mg II	2798	4.2
[Ne V]	3426	2.2
[O II]	3727	19.0
[Ne III]	3869	5.8
[O III]	4363	2.1
He II	4686n	6.3
Hβ	4861	16.5
[O III]	5007	76.9
[Fe XIV]	5303	
He I	5876	2.0
[Fe VII]	6087	0.3
[O I]	6300	2.3
[Fe X]	6375	
Hα	6563	56.5
[N II]	6583	5.1
[S II]	6731	4.0
[Fe XI]	7892	

Higher temperatures do not occur because cooling due to collisional excitation of Lyα is important if the metal abundances are low (Hummer 1963). Examination of both the model in Table 2 and many other unpublished models shows that the O^{+2} zone is ionized mainly by the radiation field between 3 and 4 Ry; this is because of the opacity of He^+ above 4 Ry, and of H^0 and He^0 between 1 and 3 Ry. It is a fairly general result. Heating is mainly due to photoionization of hydrogen, and the fraction of hydrogen that is neutral varies between $H^0/H^+ \sim 10^{-3}$–10^{-2} across the O^{+2} zone. (This result is also fairly general; it is even valid for planetary nebulae ionized by 10^5 K blackbodies.) Under these circumstances the balance between photoelectric heating and Lyα cooling gives

$$t_4 = \frac{11.83}{10.764 + 0.75 \ln t_4 + \ln (H^0/H^+)},$$

where $t_4 \equiv T_e/10^4$ K and both the H^+ recombination coefficient and Aggarwal's (1983) Lyα collision strengths are approximated as power laws in temperature, fitted over the range between 1 and 5×10^4 K. The range of neutral fraction between $10^{-3} \leq H^0/H^+ \leq 10^{-2}$ corresponds to temperatures between 1.8×10^4 K and 2.6×10^4 K. The O^{+2} zone of a photoionized gas cannot be hotter than this, for these quite simple and fundamental reasons.

c) *Optically Thick, Filamentary Nebulae*

The O III spectrum could be interpreted as resulting from the presence of O III emitting clouds with a wide range of densities. This would occur, for instance, if individual clouds were optically thick to the ionizing continuum. In this situation, low-density clouds contribute such lines as [S II] λ6720, [O II] λ3727, and [O III] λ5007, while denser clouds (which must also be closer to the source of ionizing radiation if the same levels of ionization occur) would emit mainly such lines as [O III] λ4363 and O III] λ1663. Such geometries are required for those objects in which [O I] λ6300 is broader than other forbidden lines (see De Robertis and Osterbrock 1986).

From a theoretical point of view, a model with optically thick filaments, dispersed over a wide range in radius, is unattractive because the physical problem to be solved is not well posed. It is necessary to specify how the cloud density, column density, and filling factor vary with radius. This can only be done by invoking very specific models of the kinematics and environment in the emission-line region. Steps in this direction have been taken by, among others, Shields (1978), Carroll and Kwan (1983), and Krolik and Vrtilek (1984).

We proceed by making the simplest of possible assumptions concerning the properties of the emitting gas. We use a composition appropriate for galactic H II regions (Pagel and Edmunds 1981); the specific abundances are, by number relative to hydrogen, He = 0.1, C = 3.2×10^{-4}, N = 5.0×10^{-5}, O = 4.0×10^{-4}, Ne = 8.0×10^{-5}, Mg = 4.2×10^{-5}, Si = 4.3×10^{-5}, S = 2.0×10^{-5}, A = 3.7×10^{-6}, and Fe = 5.0×10^{-6}. This mixture incorporates order-of-magnitude depletion of iron onto dust, as was suggested by the comparison of observations and predictions of models of Seyfert 2 emission-line regions (Pequignot 1984; Ferland and Osterbrock 1986).

The run of density with radius in these models is chosen to keep the ionization parameter constant, that is, $N_H \propto r^{-2}$, where r is the radius. (Here we define the ionization parameter as the ratio of densities of ionizing photons to hydrogen nuclei, rather than free electrons.) Within factors of order unity, this is equivalent to a pressure law inversely proportional to the square of the distance to the central object. This assumed density law is motivated by two considerations. First, the ionization parameter needed to fit both the outer narrow-line region and the inner broad-line region is nearly the same, of order 10^{-2} (Davidson and Netzer 1979; Ferland 1981). Second, models of the two-phase cloud–intercloud medium, such as those presented by Krolik, McKee, and Tarter (1981), predict that the cold phase will have an ionization parameter set by a pressure-balance with the Compton-heated hot phase. If this condition holds throughout the emission-line regions, the ionization parameter will tend to be constant with radius.[4] Although the assumption of constant ionization parameter is questionable, it seems to be the best we can make until a complete description of the environment in the inner regions of active nuclei is forthcoming. We choose $\log U = -1.8$, to match the (C III] λ1909)/(C IV λ1549) intensity ratio.

Cloud stability presents global constraints on the density, ionization parameter, and column density, of the filaments (Blumenthal and Mathews 1975; Mathews 1976, 1986; Ferland and Elitzur 1984; Elitzur and Ferland 1986). We assume constant pressure clouds and consider only models which are stable against disruption by radiation pressure. In particular, we consider only models in which the internally generated radiation pressure, due to trapped lines, is less than the gas pressure throughout the model. The stability requirement sharply constrains the range of possible cloud parameters (Elitzur and Ferland 1986).

We also assume that the clouds have constant column density, which we assume to be $\log N_H = 21.5$. (Although all the models did have nearly this column density, in practice, the optical depth in the Lyman continuum was kept constant at $\log [\tau_{912}] = 3.75$, to improve the numerical stability of the models between iterations.) This choice was a trade-off between smaller column densities, which produced too little [O I] emission, and larger column densities, which resulted in greater radiation pressure.

Figure 6 shows the result of the model calculations. The distance of the clouds from the central object is indicated at the top of the figure. The lower portion of the figure shows the emergent flux (ergs cm^{-2} s^{-1}) in various emission lines, divided by the hydrogen density at the inner face of the clouds. This ratio is nearly constant because of our assumption of constant ionization parameter. Recombination lines such as Lyα and the Balmer lines increase only slightly with increasing density, because of collisional excitation from the ground state. Forbidden lines such as [O III] λ5007 remain constant below their critical density, then decrease as the levels are quenched. Finally, permitted ultraviolet lines, such as C IV λ1549, increase in strength as the density increases, since these lines carry the fraction of the total cooling previously carried by the weakening forbidden lines.

[4] We note that this particular two-phase model, in which the hot phase is at the Compton temperature T_C, cannot apply to III Zw 77 because this temperature is too low; T_C is $\sim 1.2 \times 10^6$ K for the 10^{-4}–8000 Ry radiation field assumed above. The drag force of such an intercloud medium would be far too large to permit the survival of either broad-line region (BLR) or narrow-line region (NLR) clouds, and the opacity to ionizing radii would be large.

The maximum ratio of radiation to gas pressure occurring within the clouds is shown in the upper portion of the figure. It tends to increase with increasing density and decreasing distance to the central object, because the clouds grow hotter, mainly because of decreasingly efficient forbidden-line cooling, and because of the increasing importance of collisions in building up level populations. The main sources of radiation pressure in these models are Lyα (usually contributing $\sim$90% of the total) and C IV λ1549. Two regions of instability were encountered; the first was only marginally unstable (that is, the radiation pressure exceeded the gas pressure by only a few percent) and occurred between densities of 2×10^5 cm^{-3} and 2×10^6 cm^{-3}. The clouds between these densities and $\sim 2 \times 10^7$ cm^{-3} were found to be only marginally stable (that is, the radiation pressure was only a few percent below the gas pressure). Higher density clouds were completely unstable; in fact, stable solutions for the chosen column density were not possible until the broad-line region was reached ($N \geq 5 \times 10^9$ cm^{-3}) and emission-line thermalization limited the buildup of radiation pressure. (This instability provides a natural explanation for the division into broad and narrow lines.)

The observed fluxes can be predicted by integrating over the ensemble of clouds

$$I = \int N_H(r) \epsilon(r) A_C \rho_C 4\pi^2 dr ,$$

where $N_H(r) \propto r^{-2}$ is the hydrogen density at the inner face of the clouds, $\epsilon(r)$ is the ratio F/N_H given in Figure 6 (the product $N_H \epsilon$ gives the surface flux of the emission line), A_C is the surface area of the cloud, and ρ_C is the density of clouds (the product $A_C \rho_C$ is essentially the filling factor). We further assume a virial distribution of velocities (that is, $V \propto r^{-1/2}$) and an equation of continuity

$$4\pi r^2 M_C V = \text{constant} .$$

Here M_C is the mass density in emitting gas and is proportional to $A_C \rho_C N_H dL$, where $N_H dL$ is the cloud column density, which is assumed to be constant. Combining these equations, we find

$$I \propto \int \epsilon(r) r^{-3/2} dr .$$

The integration was done numerically over all narrow-line region radii which were found to be stable against disruption by radiation pressure. (The regions near $N_H \sim 10^6$ cm^{-3} and $N_H > 2 \times 10^7$ cm^{-3} were excluded.)

Table 3 gives the result of the integrations. Intensity ratios of various lines are given relative to Lyα, and their mean radius of formation are given in column (3). This model does succeed in reproducing the general features of NLR spectra. The red [S II] doublet ratio indicates a density near 2000 cm^{-3}, in agreement with typical observations (see De Robertis and Osterbrock 1986). The [O III] line ratios observed in III Zw 77 are not reproduced in detail because of our stability requirement; λ1663 increases in strength relative to the forbidden [O III] lines at smaller radii (as Fig. 6 shows). The observed relative intensity of λ1663 could easily have been matched by continuing the integration beyond the point where Lyα radiation pressure destroys clouds.

Column (5) of Table 3 gives an indication of the width of the various lines relative to Lyα. Under our assumption of a virial distribution of velocities, the width is simply proportional to

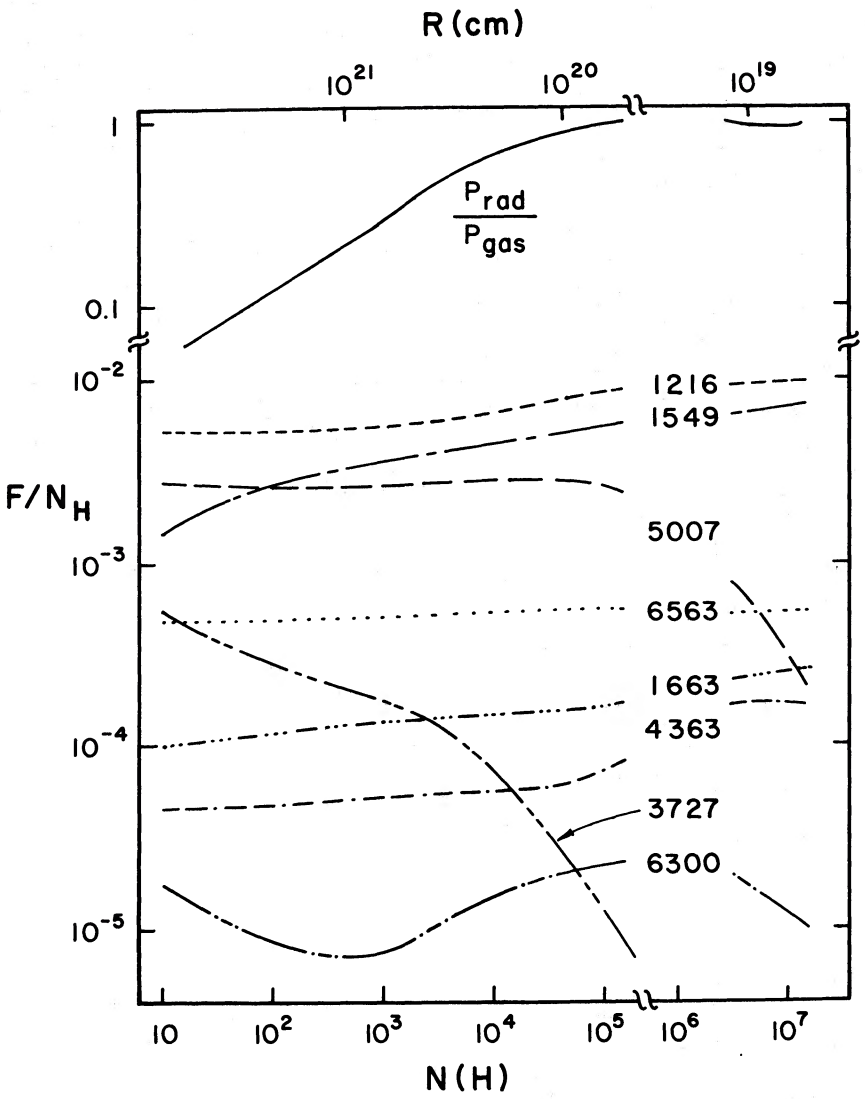

FIG. 6.—Emission-line calculations. The ratio of the flux (ergs cm^{-2} s^{-1}) in various emission lines to the hydrogen density at the inner face of the clouds is shown. The hydrogen density was varied, and constant column density and ionization parameter models were computed. The radial distance to the central photoionization source corresponding to the densities (for our choice of ionization parameter and the inferred ionizing continuum) is indicated at the top of the figure. The calculations assume constant total (gas and radiation) pressure, and the largest value of the ratio of radiation to gas pressure is indicated at the top of the figure. Models in which the radiation pressure exceeds the gas pressure are unstable; such stability problems occur near $N_H \sim 10^6$ cm^{-3} and for $N_H > 3 \times 10^7$ cm^{-3}. Clouds with the assumed characteristics cannot exist in these regions.

the square root of the mean radius of formation. (The virial mass, $M_V \sim rV^2/2G$, is $\sim 3 \times 10^8$ $M_\odot$.) The relative line widths are in general agreement with observational data. One surprising prediction is that the He I λ5876 emission produced in the NLR should be broader than He II λ4686; this is because of an increased contribution from collisional excitation of λ5876 from 2^3S in inner, denser regions of the ensemble of clouds. (Collision rates from Berrington *et al.* [1985] and a seven-level He I atom are used in this calculation of the He I spectrum.) Another prediction is that the [O I] λ6300 lines should be broader than other forbidden lines. This is in fact a general feature of NLR spectra (see De Robertis and Osterbrock 1984), although III Zw 77 is an exception to this rule (the observed λ6300 line is in fact quite sharp [Osterbrock 1981]).[5]

This model cannot reproduce the highly ionized Fe emission lines observed in III Zw 77 for two reasons. First, we have kept the ionization parameter constant across the NLR; strong Fe VII–Fe XIV emission is observed in III Zw 77 but is not predicted by model nebulae with an ionization parameter low

[5] Our assumption that the velocity is inversely proportional to the square root of the radius will be valid only if the gas moves under the influence of a central mass. If stars also affect the gravitational potential, as seems likely for radii as large as the narrow-line region, velocity could *increase* with radius. In this case emission lines formed in outer regions would have *greater* width.

TABLE 3

EMISSION-LINE INTENSITIES–MULTICOMPONENT MODEL

Ion (1)	λ (Å) (2)	$I/I(\text{Ly}\alpha)$ (3)	⟨r⟩ (cm) (4)	Width (5)
Lyαn	1216	1000.	1.81(20)	1.00
C IV	1549	663.	1.39(20)	1.14
O III]	1663	44.6	1.65(20)	1.05
C III]	1909	124.	2.51(30)	0.849
[O II]	3727	5.40	15.3(20)	0.344
[O III]	4363	15.2	1.10(20)	1.28
He II	4686	11.6	2.54(20)	0.844
Hβ	4861	22.1	2.60(20)	0.834
[O III]	5007	180.	4.73(20)	0.618
He I	5876	3.75	1.23(20)	1.21
[O I]	6300	1.80	2.11(20)	0.925
Hα	6563	65.3	2.47(20)	0.856
[N II]	6583	2.61	8.18(20)	0.470
[S II]	6731	1.21	7.60(20)	0.488
[S II]	6716	0.854	12.3(20)	0.384

enough to reproduce the observed O and C emission lines. A region with high ionization parameter is needed. A second reason is that our assumed elemental composition is appropriate for galactic H II regions; it has Fe depleted from stellar abundances by roughly an order of magnitude. Fe is usually observed to be depleted in environments where dust has formed (see Shields 1975). In fact, an order of magnitude depletion *is* necessary in order for the model to predict sufficiently weak Fe II–Fe V emission to match the observed III Zw 77 spectrum. Thus a prediction of these models is that there must be a region, between the NLR which produces the [O III] lines and the BLR, which is highly ionized, and in which Fe is not depleted.

A likely origin of the lines of the high stages of ionization is the region between the BLR and the inner region of the NLR we considered above. The [Fe XIV] λ5303 line observed in III Zw 77 has a line width roughly 2.5 times greater than the [O III] lines. If the velocity field is virial about a point mass, the [Fe XIV] width corresponds to a radius of formation some 6.2 times closer to the central object, or roughly 7×10^{19} cm. Thick clouds within this region are unstable because of internally generated radiation pressure; a disrupted cloud could fragment into low-density subclouds, which might have lower density, and hence higher ionization parameter.

According to this model Fe is present in its gas phase in this region. This brings up the question of grain survival. A simple argument shows that it is plausible for Fe to be depleted within the NLR, but present in the gas phase closer to the central object. The type of grains which contain the Fe depleted from the gas in galactic nebulae is not known, but either silicate or iron particles are potential sites. Draine and Salpeter (1979) have shown that the temperature needed to sublime 10^2 monolayers of a grain in 5×10^6 yr is given by $T_{\text{sub}} = U_0/56k$, where k is Boltzmann's constant and U_0 is the binding energy of the grain. They also give binding energies of 4.13 eV, 5.7 eV, and 7.35 eV, for iron, silicate, and graphite grains, respectively. The corresponding sublimation temperatures are 860 K, 1180 K, and 1523 K. Iron and silicate grains are fairly easy to destroy.

We have estimated the grain temperature as a function of radius using the cross sections and assumptions outlined by Martin and Ferland (1980). The grain temperature is determined by balancing direct heating by absorption of the 10^{-4}–8000 Ry continuum, and of Lyα (which is treated using the formalism developed by Hummer and Kunasz [1980]) with cooling by radiation. A Planck-averaged emissivity and an absorption cross section appropriate for 0.05 μm graphite are used; as a result the predictions are only approximate. In the neighborhood of 10^3 K the results can be approximated by $T_{\text{grain}} \approx 1130\ (r/10^{18}\ \text{cm})^{-0.334}$; iron grains would sublime within a radius of $\sim 2 \times 10^{18}$ cm, while silicates could exist as close as 10^{18} cm (see also Gaskell, Shields, and Wampler 1981). For comparison the NLR was stable to within $\sim 5 \times 10^{18}$ cm and the "classical" BLR radius for III Zw 77 is $\sim 3 \times 10^{17}$ cm. It seems plausible that Fe may be depleted in the NLR but present in the gas phase in inner regions. These considerations suggest that gas in the region between the BLR radius and the inner NLR is highly ionized and also contains gas-phase Fe. It is unable to form thick clouds, such as those found in the NLR and BLR, because of the instability due to internally generated line-radiation pressure. Iron is present in its gas phase because the equilibrium grain temperatures are above the sublimation temperatures for iron or graphite grains.

VI. DISCUSSION

Our attention was first drawn to III Zw 77 for two reasons; the first, the presence of very high stages of ionization of Fe, was discussed by Osterbrock (1981). The second was the hope that the emission-line regions which produce the forbidden and sharp permitted lines could be modeled in simple terms; the [O I] λ6300 line in this object is narrower than forbidden lines from higher stages of ionization, suggesting that a simple planetary nebula-like ionization structure, such as that considered by Ferland and Osterbrock (1986), could reproduce the spectrum. As was discussed by Ferland and Osterbrock, the alternative geometry, one in which many clouds, each optically thick to ionizing radiation, contribute to the formation of emission lines, is demanded in situations where the [O I] line is broader than other forbidden lines. This latter geometry is much more model-dependent than the former, because of additional parameters such as the column density and mass of individual clouds.

A major result of our ultraviolet observations of III Zw 77 is the fact that the O III spectrum cannot be interpreted neglecting the role of inhomogeneities. (We reject the face-value interpretation of the line intensities, viz., shock-ionization temperatures, because this galaxy obeys the equivalent-width relationships characterizing the class of active nuclei, which are thought to be photoionized.) The spectrum can readily be interpreted if O^{+2} exists in regions with many densities. This requires that the clouds exist over a wide range in radii, since only gas with certain values of this ionization parameter contribute to the O III spectrum. We are led to a model in which clouds exist over a wide range in density and separation from the central object, but in which the ionization parameter is roughly constant. The model we consider is surprisingly successful in light of the many assumptions and simplifications which went into it.

It seems clear that further progress in understanding the origin and modeling of the emission-line regions of active nuclei must involve the complete description of the properties of the gaseous environment. Such parameters as the filling factor, column density, and pressure of clouds must be specified in a constant manner. Steps in this direction have been taken by studies which specify the properties of the postulated

hot intercloud medium, but even this hypothesis seems questionable in light of the low Compton temperature of the radiation field of III Zw 77. Even such parameters as the elemental abundances must be treated as variables, because of the role of dust both in extinguishing (and making asymmetric) emission lines, and in depleting heavy elements. Several of these uncertainties could be removed with very high spatial resolution observations of nearby objects. Obtaining such data should be given the highest priority.

We are grateful to the National Science Foundation for support of this research, to G. J. F. through grant AST 85-22213, and to D. E. O. through grant AST 83-11585. The help of NASA through grant NAG-5-239 is also acknowledged.

APPENDIX

O III SPECTRA OF OTHER SEYFERT GALAXIES

A great deal of the discussion in this paper centers on interpretation of the O III spectrum of III Zw 77. Given the modest signal-to-noise ratio of *IUE* data, as well as the presence of an unidentified line at λ1650, it would be advisable to investigate the general reliability of this emission-line diagnostic.

It has been long known that the optical [O III] spectrum could be interpreted either in terms of high temperatures or high densities. The surprisingly high temperatures deduced from the O III] lines are reminiscent of these questions, which have tentatively been resolved in favor of nebular temperatures ($\sim 10^4$ K) and densities of order the critical density of the excited ^1D level ($\sim 10^5$–10^6 cm^{-3}). III Zw 77 is not the only Seyfert galaxy in which O III] λ1663 has been detected (we denote the λλ1661, 1666 doublet by λ1663 here). In this section we combine archival ultraviolet and optical spectra of other objects to study their implications for the physical conditions.

This analysis cannot be an exact one, because very few simultaneous ultraviolet–optical observations exist. In a few cases such combined observations have been obtained, but usually it is necessary to consider data obtained at widely different epochs. The entire question is even more difficult because of differential optical–ultraviolet extinction by either embedded or intervening dust. We proceed in a manner which minimizes these problems. The best evidence now suggests that the He II spectrum is close to simple case B predictions, even for conditions found in active nuclei (MacAlpine 1981; MacAlpine *et al.* 1985). If this is true, the ratio $I(\lambda1640)/I(\lambda4686)$ should be ~8–10 (see MacAlpine *et al.* 1985). We adopt 9 as the intrinsic ratio.

With this assumption

$$\frac{I(\lambda1663)}{I(\lambda5007)} = 9\,\frac{I(\lambda1663)}{I(\lambda1640)}\,\frac{I(\lambda4686)}{I(\lambda5007)}\,.$$

This removes the uncertainties due to interstellar reddening, but leaves open questions of the validity of our assumptions concerning the He II spectrum, the effects of variability, and the fact that relative intensities of lines measured with different signal-to-noise ratio and resolution might suffer any of several systematic effects.

Table 4 summarizes *IUE* observations of the intensity ratio $I(\lambda1663)/I(\lambda1640)$ in Seyfert galaxies. This ratio can be measured fairly reliably, even with *IUE* resolution and signal-to-noise ratio, because the two features lie close together and have comparable intensities. For the cases in the table where more than one intensity was measured (usually because the object is variable), the stated ratio is the mean of all the measured values, and an uncertainty is given. Table 4 also lists the ratios $I(\lambda4363)/I(\lambda5007)$ and $I(\lambda5007)/I(\lambda4686)$, based on separate optical studies. We stress that these observations were not simultaneous, and that the optical and ultraviolet data have very different velocity resolutions (usually ~300 km s^{-1} and ~1100 km s^{-1}, respectively). This is especially a problem with He II as the broad component often has significant flux, but small residual intensity. Such components were not detectable in our *IUE* observations of III Zw 77, even though our observation had above average signal-to-noise ratio (by *IUE* standards). If this object is any indication, ultraviolet data will detect mainly the narrow component, while the optical-line fluxes can easily be dominated by the broad component. In case of optical observations where deconvolutions into broad and narrow He II components of λ4686 was attempted, we have assumed that the corresponding *IUE* observations of λ1640 refer to the sharp component.

TABLE 4

[O III] SPECTRA OF SEYFERT GALAXIES

Object (1)	1663/1640 (2)	Ref (3)	4363/5007 (4)	5007/4686 (5)	Ref (6)	1663/5007 (7)	Te (8)	Ne (9)
NGC 1068	<0.1	a	0.018	30.3	f	<0.03	1.2(4)	1(5)
NGC 3516	0.125	b	0.058	0.52	g, h	1.11		
NGC 3783	0.27 ± 0.07	c	0.11	1.65	i	0.84	5.(4)	2(5)
NGC 4151	0.7 ± 0.08	d	0.028	61.9	j	0.10	1.8(4)	3(4)
NGC 5548	0.67	b	0.10	40.	g	0.15	1.5(4)	1(6)
"Mean"	0.6	e	0.04	36.	k	0.15	2.(4)	6(4)
III Zw 77	0.87	...	0.11	9.5	...	0.81	5.(4)	1(4)

REFERENCES.—(a) Neugebauer *et al.* 1980; (b) Ulrich and Boisson 1983; (c) Barr, Willis, and Wilson 1983; (d) Penston *et al.* 1981; (e) Veron-Cetty, Veron, and Tarenghi 1983; (f) Koski 1978; (g) Osterbrock 1977; (h) Anderson 1970; (i) Ward and Morris 1984; (j) Osterbrock and Koski 1976; (k) Cohen 1983.

Table 4 lists values of $I(\lambda1663)/I(\lambda5007)$ and $I(\lambda4363)/I(\lambda5007)$, deduced by normalizing the observed line ratios by our assumed $I(\lambda1640)/I(\lambda4686)$ ratio. In the case of NGC 4151, we assume that the *IUE* data refer only to the narrow component of λ1640, and use Osterbrock and Koski's (1976) deconvolution of λ4686 into broad and narrow components. Ward and Morris (1984) give λ1640 fluxes for direct comparison with their optical data on NGC 3783, and we assume their reddening-corrected spectrum and the ratio of λ1663 to λ1640 measured by Barr, Willis, and Wilson (1983) to deduce the UV–optical line ratio. For NGC 3516, unphysical values of the λ1663/λ5007 ratio (2.2) resulted from our procedure involving the He II spectrum. The problem is both the faintness of the ultraviolet O III] lines relative to λ1640 and the difficulty in measuring the λ4686 line. The value of the 1663/5007 ratio in the table is deduced by taking the absolute flux in λ5007 from Anderson (1970), the flux in λ1663 from Ulrich and Boisson (1983), and reddening of $E(B-V) = 0.22$ from DeZotti and Gaskell (1985).

III Zw 77 is included in Table 4 to facilitate comparison with other Seyfert galaxies. We also include a "mean" spectrum in the table, with ultraviolet data taken from Veron-Cetty, Veron, and Tarenghi (1983) and optical data from Cohen (1983). Veron-Cetty, Veron, and Tarenghi do not give explicit values of the ultraviolet O III]/He II ratio, but the lines are easily visible in their mean spectrum. We have estimated the intensity ratio from this mean spectrum. The mean ultraviolet ratios, and optical ratios, are combined by renormalizing the He II spectra, as described above.

The O III ratios measured in III Zw 77 are not unusual among the Seyfert galaxies; in fact, if our procedure is correct, the $I(\lambda1663)/I(\lambda5007)$ measured by us is only slightly above average. The last two columns of Table 4 give a rough indication of the deduced values of the density and temperature; these are the approximate values of the temperature and density which reproduce the observed line ratios (actually a continuum of conditions will fit individual pairs of line ratios because of the uncertainties in the analysis). It would be surprising if the $I(1663)/I(5007)$ ratios deduced here were more accurate than ~ 0.3 dex. The corresponding error in the physical conditions amounts to roughly 20% in the temperature, and 50% in the density. Surprisingly high temperatures are deduced for two galaxies, III Zw 77 and NGC 3783. The λ1663 line is too strong in NGC 3516 to be accounted for by any physical conditions. Even the lowest temperatures are high for O^{+2} zones of nebulae with solar or H II region compositions. Inhomogeneities must play some role in the formation of the O III spectrum in all of these cases.

REFERENCES

Aggarwal, K. M. 1983, *M.N.R.A.S.*, **202**, 15P.
Aldrovandi, S. M. V., and Gruenwald, R. B. 1985, *Astr. Ap.*, **147**, 331.
Anderson, K. S. 1970, *Ap. J.*, **162**, 743.
Arnaud, K. A., *et al.* 1985, *M.N.R.A.S.*, **217**, 105.
Barr, P., Willis, A. J., and Wilson, R. 1983, *M.N.R.A.S.*, **202**, 453.
Balzano, V. A., and Weedman, D. W. 1981, *Ap. J.*, **243**, 756.
Berrington, K. A., Burke, P. G., Freitas, L., and Kingston, A. E. 1985, *J. Phys. B.*, **18**, 4135.
Blumenthal, G. R., and Mathews, W. G. 1975, *Ap. J.*, **198**, 517.
Burgess, A., and Seaton, M. J. 1960, *M.N.R.A.S.*, **121**, 76.
Burstein, D., and Heiles, C. 1982, *A.J.*, **87**, 1165.
Carroll, T. J., and Kwan, J. 1983, *Ap. J.*, **274**, 113.
Cohen, R. D. 1983, *Ap. J.*, **273**, 489.
Contini, M., and Aldrovandi, S. M. V. 1983, *Astr. Ap.*, **127**, 15.
Dalgarno, A., and Sternberg, A. 1982, *Ap. J. (Letters)*, **257**, L87.
Davidson, K., and Netzer, H. 1979, *Rev. Mod. Phys.*, **51**, 715.
DeRobertis, M. M., and Osterbrock, D. E. 1984, *Ap. J.*, **286**, 171.
———. 1986, *Ap. J.*, **301**, 727.
DeZotti, G., and Gaskell, C. M. 1985, *Astr. Ap.*, **147**, 1.
Draine, B. T., and Salpeter, E. E. 1979, *Ap. J.*, **231**, 438.
Dressel, L. L., and Wilson, A. 1985, *Ap. J.*, **291**, 668.
Eastman, R. G., and MacAlpine, G. M. 1985, *Ap. J.*, **299**, 785.
Edlén, B. 1969, *Solar Phys.*, **9**, 439.
Elitzur, M., and Ferland, G. J. 1986, *Ap. J.*, **305**, 35.
Elvis, M. 1986, *Pub. A.S.P.*, **98**, 148.
Elvis, M., and Lawrence, A. 1985, *Astrophysics of Active Galaxies and Quasi-Stellar Objects*, ed. J. Miller (Mill Valley, CA: University Science Books), p. 178.
Ferland, G. J. 1981, *Ap. J.*, **249**, 17.
Ferland, G. J., and Elitzur, M. 1984, *Ap. J. (Letters)*, **285**, L11.
Ferland, G. J., and Osterbrock, D. E. 1986, *Ap. J.*, **300**, 658.
Ferland, G. J., and Shields, G. A. 1978, *Ap. J.*, **226**, 172.
Gaskell, C. M., Shields, G. A., and Wampler, E. J. 1981, *Ap. J.*, **249**, 44.
Hackney, R. L., Hackney, R. H., and Kondo, Y. 1984, in *Advances in Ultraviolet Astronomy: Four Years of IUE Research* (NASA CP 2238), p. 335.
Harrington, J. P., Seaton, M. J., Adams, S., and Lutz, J. H. 1982, *M.N.R.A.S.*, **199**, 517.
Hummer, D. G. 1963, *M.N.R.A.S.*, **125**, 461.
Hummer, D. G., and Kunasz, P. B. 1980, *Ap. J.*, **236**, 609.
Koski, A. T. 1978, **223**, 56.
Krolik, J. H., McKee, C. F., and Tarter, C. B. 1981, *Ap. J.*, **249**, 422.
Krolik, J., and Vrtilek, J. 1984, *Ap. J.*, **279**, 521.
Kwan, J., and Krolik, J. 1981, *Ap. J.*, **250**, 478.
Lambert, D. L. 1978, *M.N.R.A.S.*, **182**, 249.
Lawrence, A., and Elvis, M. 1982, *Ap. J.*, **256**, 410.
MacAlpine, G. M. 1981, *Ap. J.*, **251**, 465.
MacAlpine, G. M., Davidson, K., Gull, T. R., and Wu, C. C. 1985, *Ap. J.*, **294**, 147.
Malkan, M. A. 1984, in *X-Ray and UV Emission from Active Galactic Nuclei*, ed. W. Brinkmann and J. Trumper (MPE Report 184), p. 123.
Malkan, M. A., and Sargent, W. L. W. 1982, *Ap. J.*, **254**, 22.
Martin, P. G., and Ferland, G. J. 1980, *Ap. J. (Letters)*, **235**, L125.
Mathews, W. G. 1976, *Ap. J.*, **207**, 351.
———. 1986, *Ap. J.*, **305**, 187.
Mendoza, C. 1983, in *IAU Syposium 103, Planetary Nebulae*, ed. D. Flower (Dordrecht: Reidel), p. 143.
McGuire, E. J. 1969, *Phys. Rev.*, **185**, 1.
Miller, J. S., Robinson, L. B., and Wampler, E. J., 1976, in *Adv. Electronics Electron Phys.*, **40B**, p. 693.
Mushotzky, R. F. 1982, *Ap. J.*, **256**, 92.
Netzer, H. 1985, *Ap. J.*, **289**, 451.
Netzer, H., Elitzur, M., and Ferland, G. J. 1985, *Ap. J.*, **299**, 752.
Neugebauer, G., *et al.* 1980, *Ap. J. (Letters)*, **238**, L502.
Nussbaumer, H., and Storey, P. J. 1981, *Astr. Ap.*, **99**, 177.
———. 1984, *Astr. Ap. Suppl.*, **56**, 293.
Oke, B. B., Shields, G. A., and Korycansky, D. G. 1984, *Ap. J.*, **277**, 64.
Osterbrock, D. E. 1974, *Astrophysics of Gaseous Nebulae* (San Francisco: Freeman).
———. 1977, *Ap. J.*, **215**, 733.
———. 1981, *Ap. J.*, **246**, 696.
Osterbrock, D. E., Dahari, O., and Ekberg, J. O. 1983, *Ap. J. (Letters)*, **273**, L31.
Osterbrock, D. E., and Koski, A. T. 1976, *M.N.R.A.S.*, **176**, 61P.
Pagel, B. E. J., and Edmunds, M. G. 1981, *Ann. Rev. Astr. Ap.*, **19**, 77.
Penston, M. V., *et al.* 1981, *M.N.R.A.S.*, **196**, 857.
Pequignot, D. 1984, *Astr. Ap.*, **131**, 159.
Peterson, B. M., Crenshaw, D. M., and Meyers, K. A. 1985, *Ap. J.*, **298**, 283.
Reichart, G. A., Mushotzky, R. F., Petre, R., and Holt, S. S. 1985, *Ap. J.*, **296**, 69.
Robinson, L. B., and Wampler, E. J., 1972, *Pub. A.S.P.*, **84**, 161.
Seaton, M. J. 1978, *M.N.R.A.S.*, **185**, 5P.
———. 1979, *M.N.R.A.S.*, **187**, 73P.
Shields, G. A. 1975, *Ap. J.*, **195**, 475.
Shields, G. A. 1978, in *Pittsburgh Conference on BL Lac Objects*, ed. A. M. Wolfe (Pittsburgh: University of Pittsburgh), p. 257.
Shuder, J. M. 1981, *Ap. J.*, **244**, 12.
Stein, W. A., and O'Dell, S. L., 1985, in *Astrophysics of Active Galaxies and Quasi-Stellar Objects*, ed. J. Miller (Mill Valley, CA: University Science Books), p. 643.
Stone, R. P. S., 1974, *Ap. J.*, **193**, 135.
———. 1977, *Ap. J.*, **218**, 767.
Ulrich, M. H., and Boisson, C. 1983, *Ap. J.*, **267**, 515.

Veron-Cetty, M-P., Veron, P., and Tarenghi, M. 1983, *Astr. Ap.*, **119**, 69.
Ward, M., and Morris, S. 1984, *M.N.R.A.S.*, **207**, 867.
Weisheit, J., and Collins, L. A., 1976, *Ap. J.*, **210**, 299.
Wills, B., Netzer, H., and Wills, D. 1985, *Ap. J.*, **288**, 94.
Wilson, A. S., and Meurs, E. 1982, *Astr. Ap. Suppl.*, **50**, 217.
Wu, C. C., Boggess, A., and Gull, T. R. 1983, *Ap. J.*, **266**, 28.
Yee, H. K. C. 1980, *Ap. J.*, **241**, 894.
Zamorani, G., *et al.* 1981, *Ap. J.*, **245**, 357.

GARY J. FERLAND: Astronomy Department, The Ohio State University, Columbus, OH 43210

DONALD E. OSTERBROCK: Lick Observatory, University of California, Santa Cruz, CA 95064